

Article

# Volcanic Holocrystalline Bedrock and Hydrothermal Alteration: A Terrestrial Analogue for Mars

Anna Chiara Tangari <sup>1,\*</sup>, Lucia Marinangeli <sup>1</sup>, Fabio Scarciglia <sup>2</sup>, Loredana Pompilio <sup>3</sup>  
and Eugenio Piluso <sup>2</sup>

<sup>1</sup> Dipartimento di Scienze Psicologiche della Salute e del Territorio (DiSPUTer), Università di Chieti-Pescara, 66100 Chieti, Italy; lucia.marinangeli@unich.it

<sup>2</sup> Dipartimento di Biologia, Ecologia e Scienze della Terra (DIBEST), Università della Calabria, 87036 Arcavacata di Rende (CS), Italy; fabio.scarciglia@unical.it (F.S.); eugenio.piluso@unical.it (E.P.)

<sup>3</sup> Istituto per il Rilevamento Elettromagnetico dell' Ambiente, Consiglio nazionale delle Ricerche, 20133 Milano, Italy; pompilio.l@irea.cnr.it

\* Correspondence: a.tangari@unich.it

Received: 30 September 2020; Accepted: 28 November 2020; Published: 2 December 2020



**Abstract:** Clay minerals have been detected on Mars to outcrop mainly as alteration of ancient bedrock, and secondarily, as deposition from aqueous environments or interlayered with evaporitic deposits on Mars. In order to better constrain the alteration environments, we focused on the process to form clays from volcanic rocks and experimentally reproduced it at different temperature and pH. A fresh, holocrystalline alkali-basalt sample collected in the Mount Etna volcanic sequence has been used as analogue of the Martian unaltered bedrock. Previous works considered only volcanic glass or single mineral, but this may not reflect the full environmental conditions. Instead, we altered the bulk rock and analyzed the changes of primary minerals to constrain the minimum environmental parameters to form clays. We observed that under acidic aqueous solution (pH ~ 3.5–5.0) and moderate temperature (~150–175 °C), clinopyroxene and plagioclase are altered in smectite in just a few days, while higher temperature appear to favor oxides formation regardless of pH. Plagioclases can also be transformed in zeolite, commonly found in association with clays on Mars. This transformation may occur even at very shallow depth if a magmatic source is close or hydrothermalism is triggered by meteoritic impact.

**Keywords:** Mars; basaltic rock; clay minerals; zeolite; terrestrial analogue; lab experiment

## 1. Introduction

In the last decades, the Martian mineralogy, was investigated by different instruments onboard orbiting spacecrafts as Mars Global Surveyor (TES) (Lockheed Martin Astronautics, Denver, CO, USA) [1,2], Mars Odyssey (Lockheed Martin Astronautics, Denver, CO, USA) [3], Mars Express (OMEGA) (EADS Astrium Satellites, Paris, France) [4], and Mars Reconnaissance Orbiter (CRISM) (Johns Hopkins University Applied physics laboratory, Laurel, MD, USA) [5], in situ landers (Viking Landers and Mars Pathfinder) and rovers [6], as well as studies on the Shergottite Nakhilite and Chassignite meteorites [7]. On the whole, these observations showed that the surface of Mars is primarily composed of tholeiitic basalt, although some places are more silica-rich than typical basalt and much more similar to andesitic rocks on Earth or silica glass [7]. Hyperspectral sensors in the visible-short wave infrared regions, such as MRO-CRISM (Johns Hopkins University Applied physics laboratory, Laurel, MD, USA) and MEX-OMEGA (EADS Astrium Satellites, Paris, France), also showed the presence of different hydrated minerals, including clay minerals (such as kaolinite, illite, smectite, and chlorite) evaporitic minerals such as sulfates, carbonates, chlorides, and zeolite minerals (such as analcime, chabazite, and clinoptilolite) confirming that the Martian basaltic crust has

undergone different alteration processes (i.e., weathering, hydrothermal alteration) [8–11]. In particular, clay minerals and zeolites, having the capability of accommodating water and organic molecules in their crystalline structure, have important implication on the potential microbial habitability of the Martian surface. These minerals are mainly located at the mid-latitudes in the older terrains of Mars, spanning from early Noachian to middle Hesperian (from 4.1 to 3.3 Ga) in age (e.g., [8,10]), but we cannot rule out that they may be associated to younger deposits locally.

Zeolite was observed in dust and soils on Mars [8,10,12] in crater floor and central structures often associated to Fe–Mg phyllosilicates, such as smectites, as observed in Nili Fossae and Valles Marineris (e.g., [13]). This association suggest hydrothermal activities before/after the impact or diagenesis [11,14,15]. Clay minerals have been observed also in situ, by the NASA Spirit and Curiosity rover at the Gusev and Gale craters landing sites [6,8,16,17]. In particular, Curiosity rover, identified up to 28% smectite in places in fluvio-lacustrine mudstones at the Gale crater landing site [7]. These minerals may form through processes occurring in analogies with the Earth, such as chemical weathering, or hydrothermal alteration (volcanic or impact-induced), diagenesis or metamorphism (e.g., [18–21]). These processes may act simultaneously or alternatively, thus preventing a clear identification of different overlapping events.

Although alteration processes are reasonably faster on the Earth than Mars, due to terrestrial humid and warm climate conditions, the chemical weathering measured from Martian meteorites ranges from 1 to 4 order of magnitude slower than the slowest rates on the Earth [22]. Furthermore, the last chemical weathering processes may have occurred in the late Amazonian age (227–56 Ma) indicating the availability of liquid water on the Martian surface or shallow subsurface [23].

The formation of clays by weathering processes depends on different physico-chemical variables, such as the pH of fluid and liquid solutions, the nature of “starting” material (parent material), time of rock-water interaction, temperature, rainfall rates, drainage conditions [21].

The occurrence of weathering processes in acidic conditions potentially operating on Mars have been proposed in several studies, by either experimental works or theoretical modelling (e.g., [24–27]). Many of these studies are mostly focused on the formation of sulfate from the alteration of basaltic materials and just a few took into account clays and zeolite formation under acidic weathering of volcanic substrates (e.g., [28–32]). Moreover, they do not consider the fresh bulk rock as starting material but the basaltic glass or the synthesis of Martian simulant mixed with acidic sulfate solutions or CO<sub>2</sub> used as catalyst to promote the formation of clays and zeolites as alteration products (e.g., [13,33–38]). The use of volcanic glass facilitates the alteration process as it is an amorphous, thermodynamically unstable material, which reacts more quickly to chemical alteration [39,40]. Furthermore, the volcanic glass reaction requires low energy of activation.

The main goal of this work is to better understand and constrain the conditions required for the formation of clay minerals as alteration of volcanic bedrocks on Mars, using laboratory experiments carried out on terrestrial analogues. We reproduced experimentally at lab scale the alteration of a fresh alkaline basaltic rock collected at Etna Mount. We selected Etna Mount as a Martian analogue for the following reasons: (i) the basalts are compositionally similar to those identified in different areas of the Martian surface [41]; (ii) the volcanic morphologies such as basaltic channels, caves and lava tubes are widely exposed on the Etna active volcano and are very similar to those observed on Mars [42,43].

The novelty of this work is to experimentally simulate the alteration considering a powdered bulk composition of the fresh holocrystalline Etnean basalt as starting material and without acidic sulphates solution as catalyst, but simply mixing the basaltic fresh bulk powder with an acidic aqueous solution of HCl at pH 5.0 and 3.5, after exposure at low to moderate temperature, between 80 °C and 250 °C and monitor the alteration patina on single parent crystal for each stage.

The study of the alteration of mineral assemblages, produced under a different range of conditions (i.e., pH, temperature, and time), can provide information on the reconstruction of the environmental conditions that occurred or may still occur on Mars. This warm and humid environment is considered as potential habitable niches in which microbial life could have been initiated and sustained.

## 2. Materials and Methods

### 2.1. Geological Setting of the Terrestrial Analogue

The laboratory experiment was carried out on fresh (unweathered) basalt, collected in the surrounding area of Acireale, in the southeastern side of the Etna Mount (Sicily, southern Italy), (Figure 1a,b).

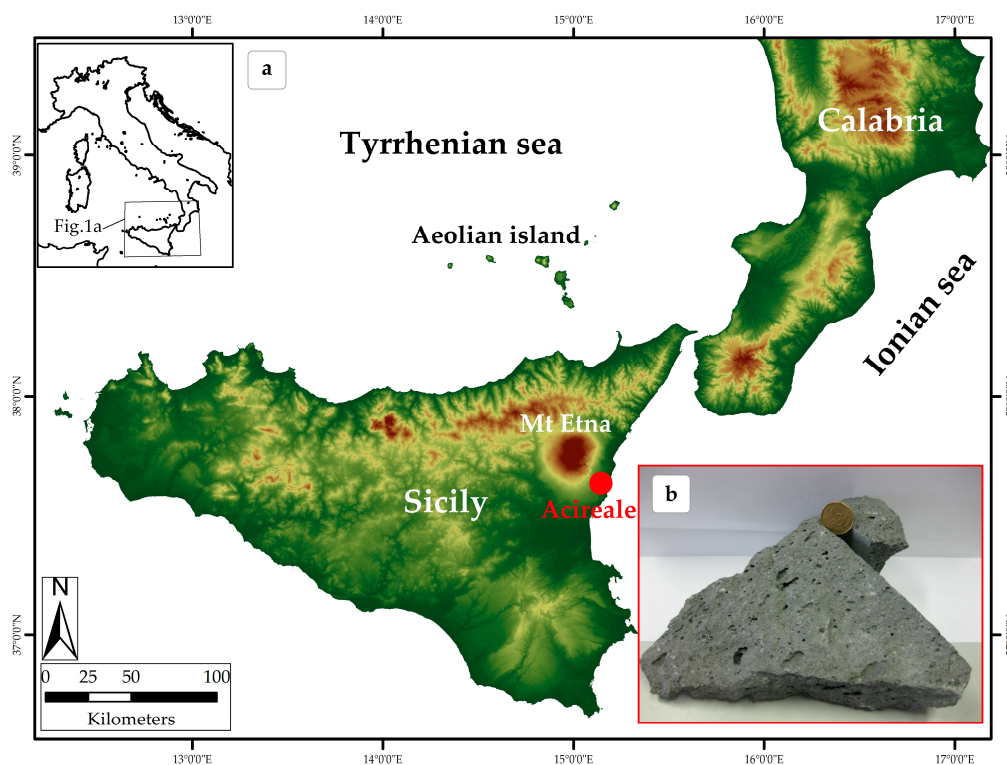


**Figure 1.** (a) Location map of the sampling site (red point) (b) Basaltic rock sample (AC1R2) collected near Acireale and used in the experiment.

The Etna Mount is a large active stratovolcano, 0.5 Ma old [44,45], located on the northeastern coast of Sicily (Southern Italy) (Figure 1a), with a maximum elevation of about 3323 m a.s.l. and influenced by warm-humid conditions typical of an upland Mediterranean climate. According to the literature [46], the Etnean basement is made of a sedimentary succession formed of, from bottom to top: (i) Maghrebic chain tectonic units and their Neogene sedimentary covers (Cretaceous-early Pliocene), (ii) marly clays sands and conglomerates (early middle-Pleistocene). The volcanic rocks are mainly composed of basaltic rocks belonging to the intermediate products of Na-alkaline basalts, hawaiitic to mugearitic in composition [47]. The basalt sample used in this study (Figure 1b) was collected from a massive lava flow about 2 m thick. Generally, this rock exhibits a greyish color with vesicles to 2 mm in size from aphanitic to porphyritic texture. The millimetric phenocrysts are made of plagioclase, pyroxene, and olivine, which are well-visible to the naked eye. This rock is included in Pietracannone formation belonging to the recent Mongibello unit, characterized by intraplate volcanism including the effusive and explosive activity of the last 15 ka [48–51]. This unit is mainly constituted by lava flow and minor pyroclastic fallout deposits [48] from basalt to mugearite composition and from aphyric to highly porphyritic texture with variable amount and size of plagioclase, pyroxene, and olivine phenocrysts [52]. Specifically, the sample rock shows an age ranged between 600 and 700 years [48]. The alkaline composition and the observable volcanic morphologies such as lava tubes and basaltic caves occurring on the Etna Mount can promote this area as an analogue for Mars.

## 2.2. Methodology

The petrography of the basalt sample was studied in thin section using a polarizing optical microscope. The total chemical composition of the major elements (as wt% oxides) was obtained using a Rigaku Supermini X-ray fluorescence spectrometer, with natural and synthetic standards with an uncertainty of 0.01%.

An amount of 400 mg of rock powder (~30 µm in size) was placed into special vessels made of Teflon and a capacity of 25 mL, and mixed with 0.8 mL of acidic aqueous solutions (at pH 3.5 and 5.0) prepared using HCl 0.015 M.

Each vessel (Figure 2) was placed into steel reactor for hydrothermal synthesis characterized by a speed heating of 5 °C/min and kept at different temperatures in a muffle furnace, as follows: 80 °C (15 days), 150 °C (for 7 and 15 days), 175 °C (15 days), 200 °C (7 days), and 250 °C (for 10 days), as indicated in Table 1.

**Table 1.** Experimental run conditions and related alteration products after AC1R2, fresh sample.

Sample	Temperature (°C)	pH	Time	Minerals Affected by Alteration	Alteration Products
AC1R2 (Acireale, Etna Mount)	80	3.5	15 days	not observed	not observed
	80	5	15 days		not observed
	150	5	7 days	clinopyroxene plagioclase	smectite
	150	5	15 days		smectite
	150	3.5	7 days		smectite
	150	3.5	15 days		smectite
	175	5	15 days		smectite, analcime
	175	3.5	15 days		smectite, analcime
	200	3.5	7 days	clinopyroxene	oxides
	250	5	10 days		oxides

Temperature and pH conditions of the aqueous solution were chosen to accelerate the alteration processes. The pressure was in equilibrium with the water vapor pressure at the corresponding temperature. We conducted this experiment at sea level pressure though the pressure on Mars is very low (6 millibars, e.g., [53]). In particular, mineralogical transformation can be considered as insensitive to the atmospheric pressure variations between Mars and Earth surface ( $10^{-3}$  bar). After each treatment, the reactors were quenched to room temperature prior to the analyses. The heated basaltic powder was then placed on the stub, with a conductive bio-adhesive scotch in carbon and metallized using a graphite coater (Q150 TES QUORUM, Laughton, UK). The scanning electron microscopy coupled with energy dispersive spectroscopy (SEM-EDS), was applied to investigate the possible neoformation of clays on the crystal surfaces and the corresponding chemical composition and morphology. A Field Emission Scanning Electron microscope FEI QUANTA 200 (Thermo Fischer Scientific, 120 Waltham, MA, USA), equipped with an EDS (Energy dispersive spectrometer) suite including a Si/Li crystal detector GENESIS-4000 (EDAX Inc., Mahwah, NJ, USA) model (EDAX, Philips Electronics, Mahwah, NJ, USA) was used. The Instrumental setup for image acquisition is as follows: 10 KeV voltage, 300 pA probe current, and work distance of 12 mm. EDS microprobe operated at a voltage between 15 and 20 kV, working distance of 10 mm, probe of 330 mA and live time of 100 seconds. The mineralogical variations after each heating treatment and the clay mineral formation were analyzed using X-ray diffractometry. Ethylene-glycol solvation was used to discriminate possible expandable clay mineral phases. Mineralogical analysis was carried out using a Rigaku MiniFlex II (Rigaku Corporation, Akishima-shi, Tokyo, Japan) diffractometer with  $\text{CuK}\alpha$  radiation, monochromated with a graphite sample and operating at 30 kV and 15 mA. XRD pattern were collected in the  $2\theta$  intervals 3–60° for

the powder sample and 3–15° for the clay minerals. Clay mineral diffraction peaks were interpreted according to Moore and Reynolds [54]. The identification of the mineral phases was performed using the Match! software (version 3.10.2) including the crystallography open database (COD 2020).



**Figure 2.** Teflon vessel and reactor for hydrothermal synthesis used in the laboratory experiment.

### 3. Results

#### 3.1. Petrography and Geochemistry of the Etnean Basalt in Comparison with Mars

Optical microscope observations of the Etnean basaltic rock (Figure 3) show a porphyritic texture composed of plagioclase, olivine, clinopyroxene, and opaque minerals set up in a holocrystalline massive intergranular microtexture groundmass. Plagioclase are euhedral and zoned from labradorite in the core to andesine in the rim and sometimes appear rounded and corroded. The clinopyroxene are diopside in composition. Olivine crystals have mainly forsterite composition. As whole phenocrysts are millimetric in size.

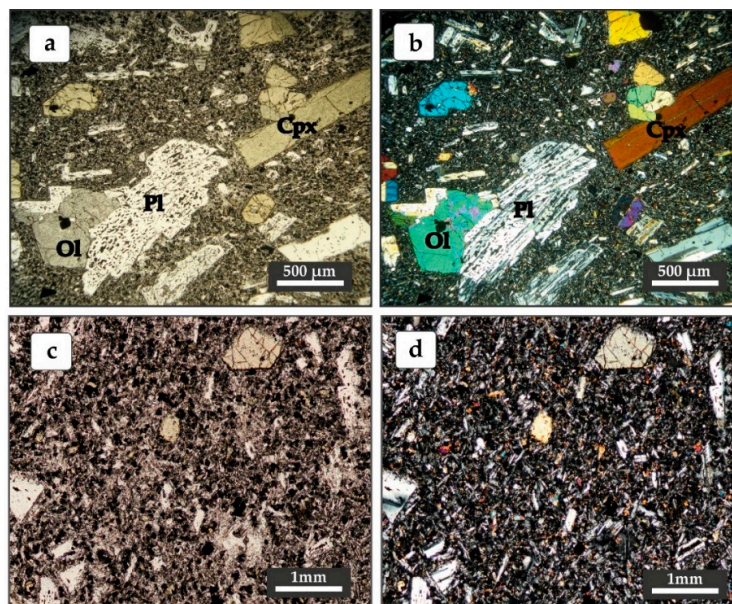


**Figure 3.** Petrography of the Etnean basaltic bedrock (sample AC1R2, Acireale site). Phenocrysts include plagioclase, clinopyroxene and olivine (a) observation in plane-polarized light (b) observation with crossed polarizers. Isotropic intergranular microtexture of the groundmass observations (c) in plane-polarized light (d) and with crossed polarizers. Pl = plagioclase; Ol = Olivine; Cpx = clinopyroxene.

The groundmass consists of small plagioclase, olivine, clinopyroxene, and opaque oxides crystals. Some glomeroporphyres made of plagioclase, olivine, and clinopyroxenes with ipidiomorphic textures can be observed dispersed in the basaltic groundmass.

The geochemistry of the sample used in this study was compared with some Martian rocks analyzed in Gale and Gusev craters landing sites on Mars as listed in Table 2. According to TAS classification diagram our sample shows a trachy-basaltic composition with an alkaline affinity (Figure 4). The TAS diagram in Figure 4 also shows the composition of Martian rocks, as derived from in situ investigations the NASA rovers Pathfinder, Spirit, Opportunity, and Curiosity and Orbiter observations from the Thermal Emission Spectrometer (TES) onboard of Mars Global Surveyor mission, as well as studies on Martian meteorites (SNC type).

**Table 2.** Chemical composition of major elements (wt%) of sample AC1R2 obtained using X-ray fluorescence and comparison with the Blackstay [54] and the Thimble basalt [55] chemical composition acquired in Gusev and Gale craters landing sites on Mars using Alpha particle X-ray spectrometer (APXS) (Jet Propulsor Laboratory, Pasadena, CA, USA) and ChemCham (Lockheed Martin Astronautics and Jet Propulsor Laboratory, USA) instrument, respectively. LOI: loss on ignition.

Major Elements	Earth		Mars	
	AC1R2 Basalt (Mount Etna)	Blackstay Basalt (Gusev Crater)	Backstay Basalt (Gusev Crater)	Thimble Basalt (Gale Crater)
SiO <sub>2</sub> (wt%)	49.07	49.50	49.50	48.79
Al <sub>2</sub> O <sub>3</sub>	19.20	13.30	13.30	14.50
MgO	3.82	8.31	8.31	4.70
Fe <sub>2</sub> O <sub>3</sub>	9.76	19.5	19.5	19.08
CaO	10.13	6.04	6.04	5.38
Na <sub>2</sub> O	4.10	4.15	4.15	4.52
K <sub>2</sub> O	1.67	1.07	1.07	1.68
P <sub>2</sub> O <sub>5</sub>	0.54	1.39	1.39	not determined
TiO <sub>2</sub>	1.52	0.93	0.93	1.23
MnO	0.17	0.24	0.24	not determined
LOI	0.53	not determined	not determined	not determined

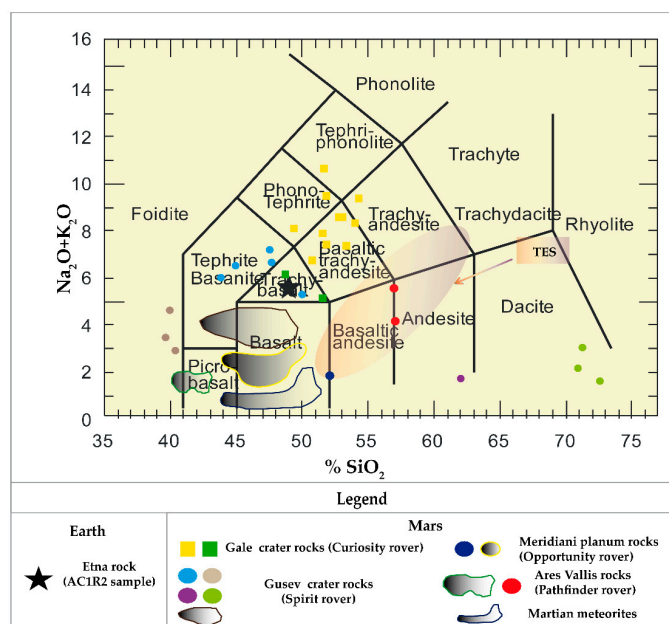


**Figure 4.** Total Alkali Silica diagram (TAS) showing the chemical composition of the Etna sample (black star) in comparison with composition of the Martian rocks so far estimated, from rover, orbiter and meteorite analyses as summarized by [7,55,56]. Thermal Emission Spectrometer (TES) is related to the measurements of rocks and soils on Mars carried out using the Thermal Emission Spectrometer onboard Mars Global Surveyor orbiter.

### 3.2. Experimental Alteration

At the SEM-EDS observation, plagioclase, clinopyroxene, olivine, and small amounts of magnetite and ilmenite in fresh rock sample show smooth surfaces, with features of physical breakage, likely caused by the mechanical crushing occurred during the sample preparation (Figure 5a). Table 1 lists the results, in terms of neo-formed minerals, for each experimental run. At SEM-EDS observation, the powder heated at 80 °C for 15 days, in acidic solutions at 3.5 and 5.0 pH, only showed mechanical breakage features on the grain surface of clinopyroxene, plagioclase and olivine (Figure 5b). Neither dissolution or neogenic products have been observed.

The heating treatment at temperature of 150 °C and acidic solution at pH 5.0 and 3.5, after 7 and 15 days produced the early formation of thin alteration coatings. The same result is also observed at 175 °C and pH 5.0. After these treatments, the alteration coatings were better developed on the clinopyroxene crystal surfaces than plagioclase grains (Figure 5c,d). They generally exhibited a “honeycomb” morphology, which became clearer with increasing temperature and acidic conditions. This was confirmed by the experimental run at 175 °C and extremely acidic pH conditions at 3.5, after seven days, which produced a coating entirely covering the clinopyroxene grains (Figure 5g) and an increase of the alteration films on the plagioclase surfaces. A change in color from gray to red of the basaltic powder was also macroscopically observed at the end of this experimental run. The red color was induced by the early growth of iron oxy-hydroxides on the crystal grains, which were not well visible due to their very small size. These oxy-hydroxides are well observed after the experiments at 200 °C and 250 °C showing the growth of Fe-Ti oxide grains with relatively low contents in Mn and Ti (not exceeding 2 wt%) on clinopyroxene. These chemical data indicate the crystallization of ilmenite with a minor pyrophanitic component. In Table 3 we report in situ EDS compositional analysis for the clinopyroxene and for the coatings developed on it, at the end of heating treatments at 150 °C and 175 °C.

As a result, EDS analyses cannot unambiguously resolve the occurrence of neo-formed minerals, which are otherwise very well shown at the morphological observation with SEM magnification. Nevertheless, the increase of Al, Mg, Fe, and Na in the coatings at the expense of Si and Ca may suggest the occurrence of an alteration process of the parent crystals.

XRD analyses of powders after heating treatments at 175 °C and pH 5 and 3.5 of the solutions, show the mineralogical transformation with the appearance and persistence of diffraction peaks around 5.61 Å and 5.13 Å, typical of zeolite minerals such as analcime (Figure 6a). In addition, the same powder heated at 175 °C in the more acidic solution at pH 3.5 shows a very weak basal reflection around 14 Å, which shifted to 17 Å after ethylene glycol solvation (Figure 6b), thus suggesting the neo-formation of smectite, in accordance with the honeycomb morphology observed using SEM.

**Table 3.** Mean values of the major elements (wt%) of clinopyroxene phenocrysts in comparison with the patina of alteration developed on it, as obtained using the EDS analysis.

Major Elements	Phenocryst of Clinopyroxene	Patina of Alteration
SiO <sub>2</sub> (wt%)	52.46	42.39
Al <sub>2</sub> O <sub>3</sub>	5.63	6.42
MgO	14.86	17.17
Fe <sub>2</sub> O <sub>3</sub>	7.56	17.98
CaO	17.51	13.34
Na <sub>2</sub> O	1.15	1.50

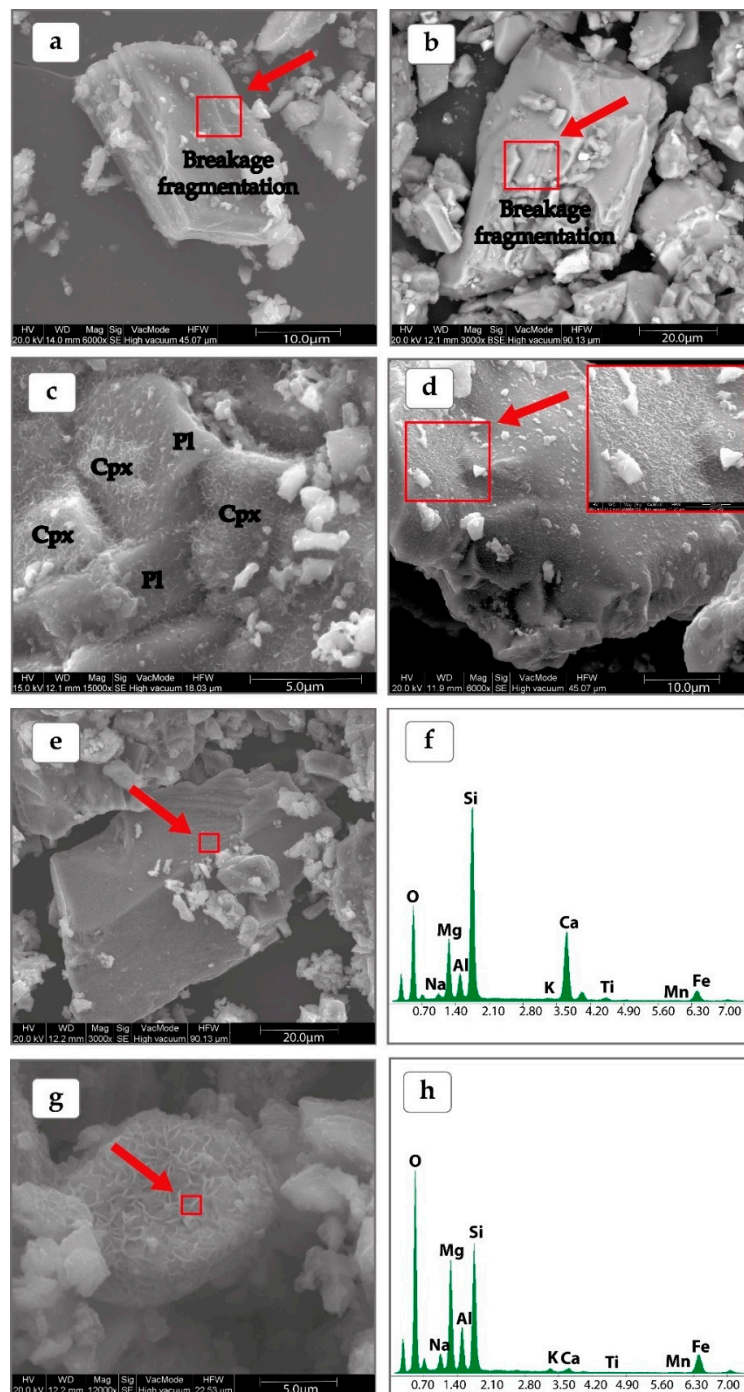


**Figure 5.** SEM images of a few crystals, before and after treatments: (a) traces of mechanical erosion on unaltered plagioclase (b) traces of breakage fragmentation (red square) on clinopyroxene, after 80 °C treatment, at pH 3.5 (back scattered image) (c) Cpx—Pl mixed grain, after 7 days heating at 150 °C in 5.0 pH, showing the early formation of clay coatings on both crystals (d) “honeycomb” morphology of the clay coating developed on a clinopyroxene crystal after heating at 150 °C and zoom in the red square (e) Coatings developed on a clinopyroxene crystal, after heating at 175 °C in the strongly acidic condition at pH 3.5 (f) EDAX spectrum acquired in the red square area of picture (e) (g) clay neo-formation with “honeycomb” morphology entirely covering the clinopyroxene crystal surface at 175 °C and pH 3.5 (h) EDS spectrum related to the red square area of picture (g) (a,c–e,g) morphological images. Cpx = clinopyroxene; Pl = plagioclase.

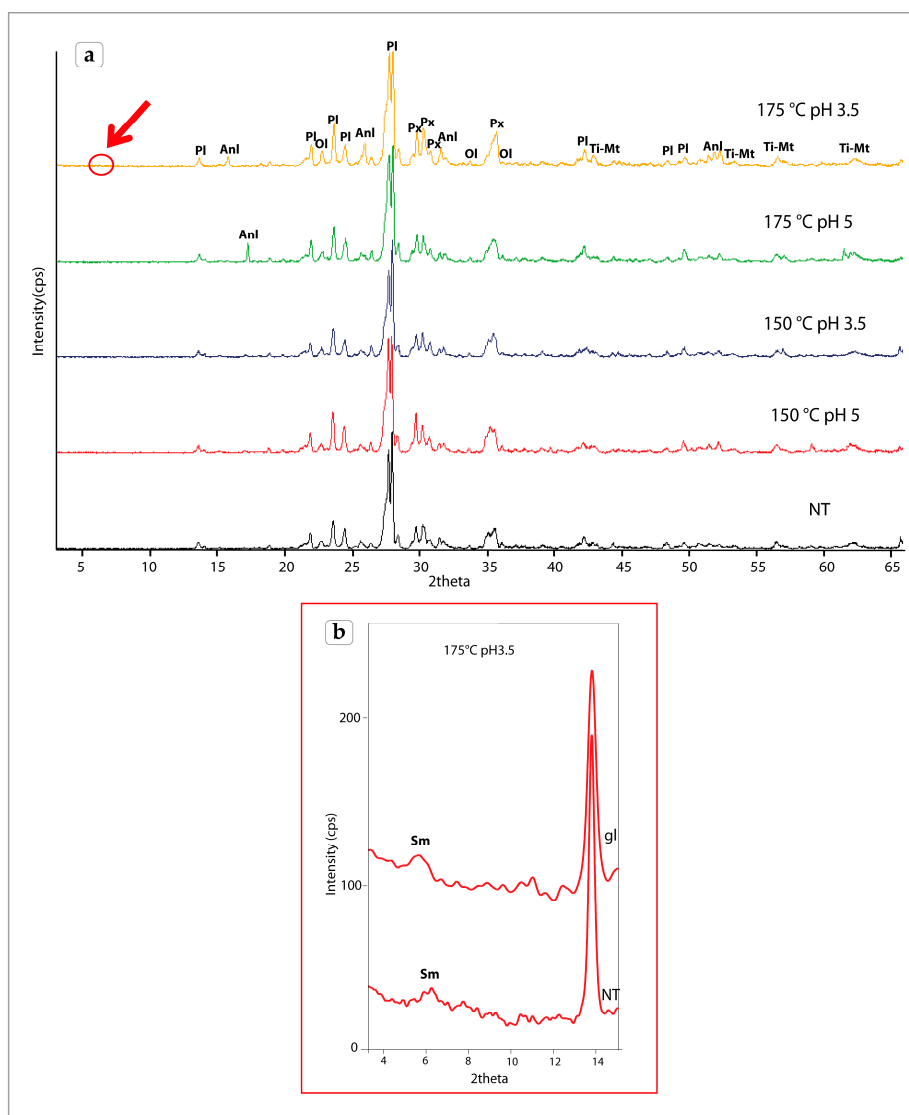


**Figure 6.** (a) XRD patterns of the sample powders, after different treatments. In comparison with the unaltered sample (black line), all the heated samples show a progressively decreasing intensity with temperature and acidity, of the diffraction peaks attributable to the main primary minerals as plagioclase (Pl), pyroxene (Px) olivine (Ol), and titanomagnetite (Ti-Mt) and the appearance of features diagnostic of both analcime (Anl) and smectite (Sm) (b) Zoom of the  $2\theta$  interval around  $6^\circ$  (red circle) of the XRD pattern measured after the treatment at  $175^\circ\text{C}$  and  $\text{pH} = 3.5$  in the figure a showing the appearance of a diffraction peak at  $14\text{ \AA}$ , typical of clay minerals. The expansion of this peak to  $17\text{ \AA}$  after ethylene glycol solvation, point out the occurrence of smectite (Sm). NT =  $175^\circ\text{C}$ , at  $\text{pH} 3.5$  untreated; gl = ethylene glycol. All the treatments shown here have been accomplished for 15 days.

## 4. Discussion

### 4.1. Mars vs. Earth Mineralogical Analogies

So far, mineralogical investigations on Mars from remote and in situ observations of soils and dunes fields have shown mainly a widespread basaltic composition [7,57] with diagnostic features of clay minerals and zeolites, suggesting the occurrence of rock–fluid interaction during time. Several orbital missions, including Mars Reconnaissance Orbiter and Mars Global Surveyor, have identified mostly alkaline basalts at the surface of Mars [1,2,58] as well as the presence of olivine, pyroxene, and plagioclase. This has been confirmed by in situ measurements of the Viking, Mars Pathfinder, and Curiosity landers

and rovers [59,60], as well as studies on the SNC meteorites [7,8]. Therefore, the basalt sample collected in the Acireale area (Etna Mount) composed of plagioclase, clinopyroxene and olivine with an alkaline geochemical affinity, suggests that it can be considered as a good analogue of the Martian crust (Figure 4). Specifically, this rock shows good analogy in terms of bulk geochemistry with the Backstay and the Thimble trachy-basaltic rocks analyzed in the Gusev and Gale craters landing sites by the rovers, as showed in Table 3.

On Mars, in addition to the alkaline basalts, tholeiitic basalts very similar in composition of bulk rock and alteration phases (as clays and zeolites) to alkaline rocks, were also detected (e.g., [32,38]). In particular, the literature of the experimental alteration of tholeiitic basalts, focuses on the glass (e.g., [32,38]), representing a thermodynamically unstable phase, which reacts very quickly to chemical alteration. Our experimental data obtained from the alteration of alkaline basaltic rock show a good agreement between the mineralogical phases produced from the alteration of crystal grains and glass. Nevertheless, the main difference involves the volumetric abundance of alteration products, which is larger on the glass than crystals, such as clinopyroxene and plagioclase. Phyllosilicates and zeolites observed with CRISM (Johns Hopkins University Applied physics laboratory, Laurel, MD, USA) and OMEGA (EADS Astrium Satellites, Paris, France) imaging spectrometers in different regions on Mars [8–10] include several clay minerals such as chlorite, vermiculite, allophane (poorly crystalline clay) serpentine, and some phyllosilicates belonging to the smectite group, such as saponite and nontronite, as well as different types of zeolite such as analcime, chabazite, and clinoptilolite. On Earth, these clays are typical weathering products of feldspars and/or pyroxene and vermiculite may also derive from K-mica and chlorite (e.g., [61–63]). Kaolinite, halloysite and allophanic components are usually promoted by the weathering and pedogenic processes in volcanic environments in humid climate but well-drained soil moisture conditions (e.g., [64–66]), and are often related to the alteration of basaltic volcanic glass in aqueous solutions [67]. Nevertheless, the alteration of volcanic glass to clay minerals has been investigated also in hydrothermal contexts [68,69]. Hydrothermal processes involving volcanic glass mainly produce the following trend of alteration: glass → imogolite-like → allophanes → halloysite → kaolinite, according to observations in soils developed in different sectors of Etna (e.g., [67,70]). However, phyllosilicates and poorly crystalline clays, may often represent the products of hydrothermal alteration. Allophane forms on the surface of volcanic glass during the earliest stages of alteration, often followed by smectite (e.g., [71]). The latter is typical of volcanic environments (e.g., [72,73]) and overall low temperatures commonly < 200 °C, also favorable to halloysite and kaolinite [20] whereas the serpentine (chrysotile-lizardite) is a typical hydrothermal alteration product of olivine [74]. The analcime is a typical hydrothermal alteration product after glass in volcanic materials at temperatures between 150 °C and 200 °C under acidic pH conditions [28,75]. Obviously, the main alteration products are also controlled by the alkaline or acidic conditions, along with the availability and relative abundance of alkalis and alkaline earths against hydrogen ions [20]. The contents of Si and Al, all sourced by the parent rock or the circulating fluids, may also have played a role. Our experimental design was also performed taking into account the hydrothermal settings present in different active volcanoes (e.g., [76–80]).

#### 4.2. *Insight into Alteration Processes from the Experimental Data*

Several previous studies provide information on conditions of alteration processes on volcanic rocks leading to the formation of clay minerals and zeolites, and constraints for different physical parameters as temperature and pH. This literature mainly focuses on the alteration of glass as starting material [8,13,34–39,71]. The laboratory experiments performed on the Etnean basalt point out an increase of the alteration degree with increasing temperature and acidic pH of the aqueous solution considering the bulk composition of the fresh holocrystalline basaltic rocks. Nevertheless, our study shows a simultaneous reaction of the glass and crystal. We showed that the temperature and pH influence the kinetics of the chemical reaction rather than time and pressure which is too low for triggering the mineralogical transformation. These alteration processes led to the development of coatings with

“honeycomb” morphology, which are more developed on the crystal grains of clinopyroxene than plagioclase. On the other hand, the olivine crystal transformation at relatively low temperature produce the growth of serpentine and minor magnetite in good agreement with the literature (e.g., [75]). The temperature which induced effective chemical and morphological changes was between 150 °C and 175 °C.

On the whole, the chemical data showed a cations mobilization of MgO, Fe<sub>2</sub>O<sub>3</sub>, Al<sub>2</sub>O<sub>3</sub>, CaO, and Na<sub>2</sub>O during the alteration process mainly on the clinopyroxene crystal as observed in Figure 7. Specifically, this data show an increase of Al<sub>2</sub>O<sub>3</sub>, MgO, Fe<sub>2</sub>O<sub>3</sub>, and Na<sub>2</sub>O contents from the clinopyroxene crystal (Figure 7a,c,e,g) to the patina developed on it (Figure 7b,d,f,h). This behavior, together with the honeycomb morphology of coatings (Figure 5c,d,g), is consistent with the formation of expandable clay minerals such as smectite. In particular, the increase of MgO and Fe<sub>2</sub>O<sub>3</sub> in the patina (Figure 7b) is in line with the formation of smectite mineral such as Fe–Mg saponite. The formation of this clay is also well observed on the coating developed at 175 °C and pH 3.5 as shown in Figure 5h. The decrease of CaO (Figure 7f) in the patina in some cases in association with a decrement of MgO and Al<sub>2</sub>O<sub>3</sub> and an increment of Fe<sub>2</sub>O<sub>3</sub>, suggests the formation of Oxy-hydroxides likely ilmenite. Furthermore, low concentrations of K<sub>2</sub>O (Figure 5h) also indicate the presence of illite, likely interstratified with the dominant expandable clay minerals, which usually form at intermediate to low temperatures [20]. However, it was often very difficult to separate the effective composition of the mineral grains from the related clay coatings, due to the very thin thickness of the latter. These experiments provide further insights into the understanding of the process of formation of alteration clay coatings on minerals. Particularly the experimental setup with increasing temperature conditions mimics hydrothermal alteration processes with temperature between 150 °C and 175 °C and acidic solutions with pH ranged between 5 and 3.5, leading to the formation of clay minerals, such as Fe–Mg saponite.

The formation of smectite is also in accordance with the honeycomb morphology and X-ray diffraction analyses, which shows a decrease in the intensity of the diffraction peaks diagnostic of pyroxenes and plagioclases with respect to the untreated material (Figure 6a). Furthermore, the appearance of the smectite diffraction peak is well observed (Figure 6b) in our sample. At the same temperature conditions also the presence of a zeolite mineral such as analcime, can be observed according to the experimental results from other authors e.g., [28,71]. The formation of analcime is probably related to the alteration of plagioclase as showed in Figure 8 where the amount of Na<sub>2</sub>O and Al<sub>2</sub>O<sub>3</sub> exhibit an increase from the crystal grain (Figure 8a) to the patina (Figure 8b). This alteration process probably occurs on the small size plagioclase included in the groundmass, since no morphological evidence of analcime on the phenocrysts to the SEM microscope was observed.

On Mars, analcime was observed in the deposits around the central peaks of impact craters located in Nili Fossae and Isidis Planitia, often in association with Fe/Mg phyllosilicates (i.e., smectite), thus suggesting a post-impact hydrothermal alteration [15]. Previous experimental alterations of tholeiitic glass in aqueous environment, with variable CO<sub>2</sub> concentrations [13] reproduced this association, showing that a decrease of CO<sub>2</sub> content, reduces the smectite amount more efficiently than the zeolite, which prevails in alkaline pH > 8.2 [13].

As already mentioned in the previous paragraphs, the presence of smectite in different regions on Mars has been widely observed using orbiter and in situ data (e.g., [8,17,81]). Therefore, it is reasonable that some processes of alteration of the original basalt due to warm and acid fluids could have leads to the formation of smectite on Mars, similarly to our Etnean sample under experimental conditions. Different studies simulate the formation of smectite from alteration of volcanic glass sand simulants mixed with acid sulfate solutions or CO<sub>2</sub> [33–38]. In this respect, the experimental conditions (temperature and pH) used in our study mimic a hydrothermal alteration process with formation of smectite. The formation of smectite in hydrothermal environments is plausible on Mars, since evidence of hydrothermal activity has been widely observed in Gusev crater, such as soils likely formed as fumarole or oxidative alteration of Fe/sulphates deposits [82].

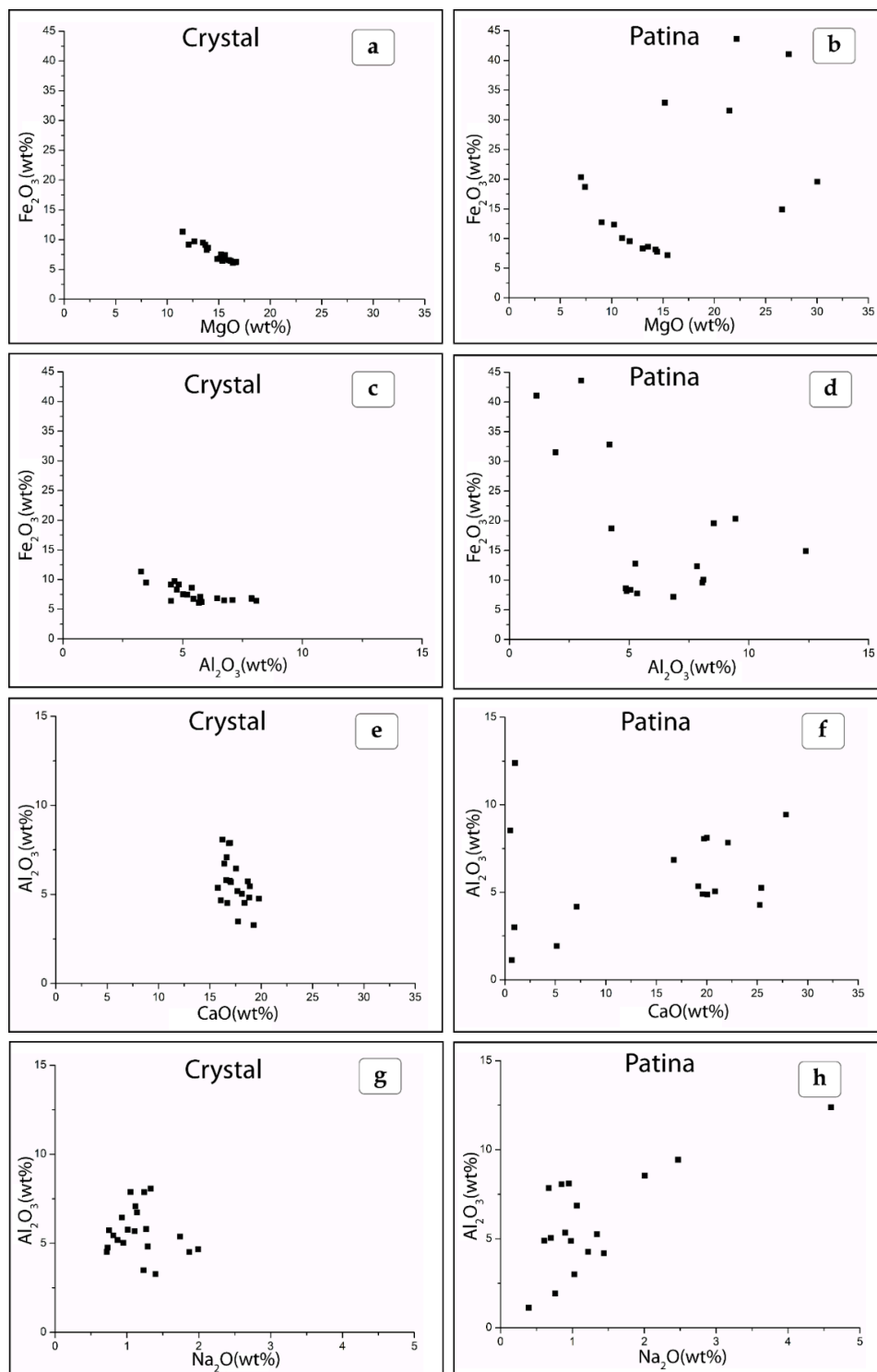


**Figure 7.** The scatter plot shows the cation mobilization of MgO, Fe<sub>2</sub>O<sub>3</sub>, Al<sub>2</sub>O<sub>3</sub>, CaO, and Na<sub>2</sub>O from the crystal to the patina developed on it, during the alteration process on the clinopyroxene grains at temperature of 150 °C and 175 °C and pH 5 and 3.5, respectively. (a,c,e,g) Diagrams showing the composition of clinopyroxene crystals where the absence and the incipient formation of the patina respectively occur (b,d,f,h) Scatter plot showing the mobilization of the chemical elements in the patina developed on clinopyroxenes. The chemical elements indicate a clear increase of (d) Fe<sub>2</sub>O<sub>3</sub> and Al<sub>2</sub>O<sub>3</sub>, coupled in more cases with (b) which indicates the formation of smectite as Fe–Mg saponite.

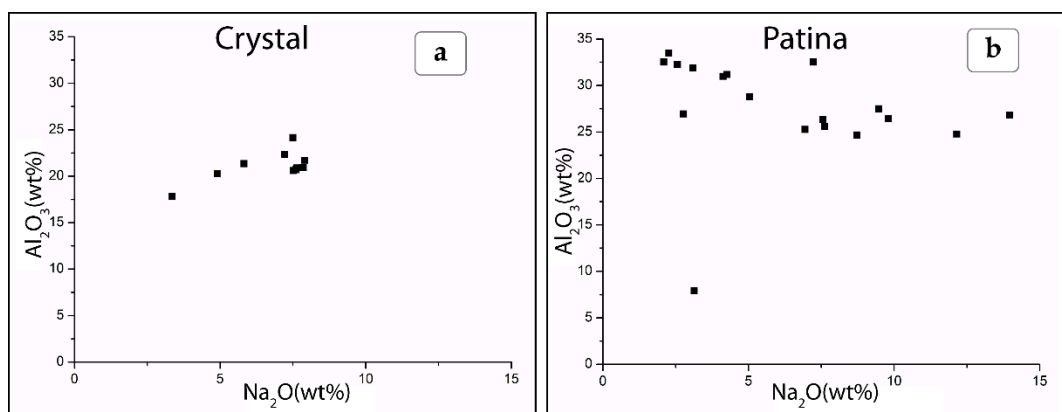


**Figure 8.** Diagrams show the cations mobilization of  $\text{Na}_2\text{O}$  and  $\text{Al}_2\text{O}_3$ , from the crystal to the patina developed during the alteration process affecting the plagioclase grains at temperature of  $150\text{ }^\circ\text{C}$  and  $175\text{ }^\circ\text{C}$  and pH 5 and 3.5, respectively. (a) Diagrams showing the composition of the plagioclase. (b) B-plot showing clear increase of  $\text{Na}_2\text{O}$  and  $\text{Al}_2\text{O}_3$  in the patina developed on plagioclase.

Although our experimental setup favor the hydrothermal alteration as responsible for the formation of the smectite clay, also the role of chemical weathering also suggested in different regions on Mars cannot be excluded (e.g., [8,16,17,81,83]). Several studies proposed geomorphological evidence based on numerous and well-preserved valley networks and channels, and many impact craters that show deltas, lakes and sedimentary layers (e.g., [81,84,85]), coupled with a hydrated mineralogy, which suggest an ancient water–rock interaction (e.g., [8]), which may have contributed to the neogenesis of smectite under environmental meteoric conditions. Specifically, the chemical weathering processes in the Gale and Gusev craters on Mars where the alkaline basalts outcrop, induced the formation of smectite in analogies with the Etna basaltic sample (see Section 3.1) [16,83,86,87]. Nevertheless, simulation of the weathering processes requires longer time ranges of exposure of the basalt parent rock to fluid–rock interaction, as normally happens in terrestrial conditions. Therefore, in the laboratory high temperature is required to speed up the weathering reactions, since lower temperatures require longer timescales to appreciate the effects of chemical and mineralogical transformations. Moreover, acidic aqueous solutions (pH between 3.5 and 5) provide  $\text{H}^+$  ions which accelerate the chemical exchange in the reactions, thus triggering the alteration processes. Although weathering processes are reasonably fast under the Mediterranean climate, and in particular the temperate to warm and humid climate typical of Mount Etna, also slightly acidic conditions induced by the decomposition of the organic matter may accelerate these processes, as observed in many other environments [88]. Similar pH values of the solutions used for our experiment were measured in a volcano-sedimentary complex of the Rio Tinto River (Spain) subjected to an intense hydrothermal mineralization. There, the acidic water related to a high amount of biomass, increased the weathering rate, and forms several clay minerals such as smectite, illite, and kaolinite [89]. In that area, smectite was promoted in a volcanoclastic andesite and sedimentary fluvial and lacustrine deposits [89]. Moreover, geothermal systems in active volcanoes as hot springs, and mud pools also produce sulphates, which can provide similar temperature and acidic conditions ( $\text{pH} \leq 5$ ) to our experimental setup used for the Etnean sample [77–80]. In particular, the formation of smectite which preserves a microbial signature is well observed in hydrothermal systems of hot springs [76,90]. Caves and lava tubes represent other environments where the preservation of microbial biosignatures, or traces of life, in mineral deposits also occur [43].

In comparison with Mars the formation of smectite minerals was also well investigated in the Columbia Hills at the Gusev crater, where the morphological and mineralogical evidence of hydrothermal alteration are well exposed [91,92]. The smectite observed include saponite [93,94] which is a typical product of the hydrothermal alteration in line with the smectite formed in our experiment.

Alteration processes on Mars obviously required a longer time considering the plate tectonic absence and the actual cold and dry climate with low temperature at the surface, ranging from 140 and 310 K [95]. Alteration processes under acidic conditions on Mars leading to clay mineral formation are supported by different authors (e.g., [30,32,96,97]) invoking extremely to slightly acidic pH of fluids. The potential source of acidity could have been the volcanic activity, which induced the release of high contents of CO<sub>2</sub> and SO<sub>2</sub> in the atmosphere thus producing the condensation of water vapor and acid gases that interact with the basaltic bedrock and produced alteration minerals [98]. These acidic conditions were likely superimposed to warm and humid conditions, according to Halevy and Head [99], similarly to what we observe today on Mount Etna. The presence of hydrogen peroxide, which is a strong oxidant agent, and widely detected in the present-day Martian atmosphere [100] could have been a further source of acidity.

## 5. Conclusions

We performed a laboratory experiment on the fresh holocrystalline alkaline basaltic rock collected on Mount Etna to better understand and constrain the conditions required for the formation of clay minerals on Mars. This analogue shows a good similarity with the basaltic rocks outcropping in the Gale and Gusev landing sites in terms of bulk mineralogy, chemistry. Laboratory experiments carried out on the bulk of the holocrystalline fresh basaltic powder, under different conditions of acidity of fluids water (pH of 5 and 3.5), temperature (between 80 °C and 250 °C) and time (between 7 and 15 days), promoted the formation of clay minerals as coatings on the parent crystal and zeolites in a few days. In particular, the heating of acid aqueous solutions up to temperature between 150 °C and 175 °C produced the formation of coatings with “honeycomb” morphology typical of smectite (as Fe–Mg saponite) on the surface of clinopyroxene and plagioclase crystals, just in a few days. The cations mobilization from the crystal to the patina indicates the development of coatings faster and more efficient on clinopyroxene than plagioclase where the formation of analcime (zeolite) occurs. Furthermore, temperature above 175 °C seems to favor the formation of oxides rather than clays, regardless the pH. The results of our work suggest that on Mars, environmental conditions to produce clays can be reached in a limited range of T and pH with acidic fluids (probably deriving from the volcanic activity in a warm and humid climate or by oxidation of the groundwater on the surface), and the alteration of the basaltic bedrock can occur at shallow depth if a source of heat (volcanic or impact) is close enough to reach the optimum temperature range. Finally, this work demonstrates that the basaltic rocks of Etna can be considered as a good Martian analogue to model the weathering processes.

**Author Contributions:** Data curation, A.C.T.; Formal analysis, A.C.T.; Investigation, A.C.T.; Methodology, A.C.T.; Software, L.P.; Supervision, L.M., F.S., and E.P.; Writing—original draft, A.C.T.; Writing—review & editing, A.C.T., L.M., F.S., L.P., and E.P. All authors have read and agreed to the published version of the manuscript.

**Funding:** This research received external funding from the Italian Space Agency, contract n. 2015-036-R.0.

**Acknowledgments:** The authors are grateful to A. Bloise for Experimental Mineralogy laboratory facilities at the University of Calabria. The authors thank M. Davoli (University of Calabria) for his help during SEM-EDS analyses. We wish to thank D. Cirillo (University of Chieti-Pescara) for his help with the use of ArcGIS software package. We are grateful to three anonymous reviewers and the guest editor, whose constructive comments helped us to improve the quality of our work.

**Conflicts of Interest:** The authors declare no conflict of interest.

## References

1. Hamilton, V.E.; Christensen, P.R.; McSween, H.Y., Jr.; Bandfield, J.L. Searching for the source regions of martian meteorites using MGS TES: Integrating Martian meteorites into the global distribution of igneous materials on Mars. *Meteor. Planet. Sci.* **2003**, *38*, 871–885. [[CrossRef](#)]
2. Wyatt, M.B.; McSween, H.Y. Spectral evidence for weathered basalt as an alternative to andesite in the northern lowlands of Mars. *Nature* **2002**, *417*, 263–266. [[CrossRef](#)]

3. Saunders, R.S.; Arvidson, R.E.; Badhwar, G.D.; Boynton, W.V.; Christensen, P.R.; Cucinotta, F.A.; Feldman, W.C.; Gibbs, R.G.; Kloss, C., Jr.; Landano, M.R.; et al. 2001 Mars Odyssey mission summary. *Space Sci. Rev.* **2004**, *110*, 1–36. [[CrossRef](#)]
4. Bibring, J.P.; Langevin, Y.; Mustard, J.F.; Poulet, F.; Arvidson, R.; Gendrin, A.; Gondet, B.; Mangold, N.; Pinet, P.; Forget, F. Global mineralogical and aqueous Mars history derived from OMEGA/Mars Express data. *Science* **2006**, *312*, 400–404. [[CrossRef](#)]
5. Murchie, S.L.; Arvidson, R.; Bedini, P.; Beisser, K.; Bibring, J.P.; Bishop, J.; Boldt, J.; Cavender, P.; Choo, T.; Clancy, R.T.; et al. Compact Reconnaissance Imaging Spectrometer for Mars (CRISM) on Mars Reconnaissance Orbiter (MRO). *J. Geophys. Res.* **2007**, *112*, E05S03. [[CrossRef](#)]
6. Bristow, T.F.; Rampe, E.B.; Achilles, C.N.; Blake, D.F.; Chipera, S.J.; Craig, P.; Crisp, J.A.; Des Marais, D.J.; Downs, R.T.; Gellert, R.; et al. Clay Mineral Diversity and Abundance in Sedimentary Rocks of Gale Crater, Mars. *Sci. Adv.* **2018**, *4*, eaar3330. [[CrossRef](#)]
7. McSween, H.Y. Petrology on Mars. *Am. Mineral.* **2015**, *100*, 2380–2395. [[CrossRef](#)]
8. Ehlmann, B.L.; Edwards, C.S. Mineralogy of the Martian Surface. *Annu. Rev. Earth Planet. Sci.* **2014**, *42*, 291–315. [[CrossRef](#)]
9. Ehlmann, B.L.; Mustard, J.F.; Murchie, S.L.; Bibring, J.-P.; Meunier, A.; Fraeman, A.; Langevin, Y. Subsurface water and claymineral formation during the early history of Mars. *Nature* **2011**, *479*, 53–60. [[CrossRef](#)]
10. Carter, J.; Poulet, F.; Bibring, J.; Mangold, N.; Murchie, S. Hydrous minerals on Mars as seen by the CRISM and OMEGA imaging spectrometers: Updated global view. *J. Geophys. Res.* **2013**, *118*, 831–858. [[CrossRef](#)]
11. Sun, V.Z.; Milliken, R.E. Ancient and recent clay formation on Mars as revealed from a global survey of hydrous minerals in crater central peaks. *J. Geophys. Res. Planets* **2015**, *120*, 2293–2332. [[CrossRef](#)]
12. Ruff, S.W. Spectral evidence for zeolite in the dust on Mars. *Icarus* **2004**, *168*, 131–143. [[CrossRef](#)]
13. Viennet, J.C.; Bultel, B.; Riu, L.; Werner, S. Dioctahedral phyllosilicates/zeolites versus carbonates/zeolites competitions as constraints to understand early Mars alteration conditions. *J. Geophys. Res. Plan.* **2017**, *122*, 2328–2343. [[CrossRef](#)]
14. Viviano-Beck, C.E.; Murchie, S.L.; Beck, A.W.; Dohm, J.M. Compositional and structural constraints on the geologic history of eastern Tharsis rise, Mars. *Icarus* **2017**, *284*, 43–58. [[CrossRef](#)]
15. Ehlmann, B.L.; Mustard, J.F.; Swayze, G.A.; Clark, R.N.; Bishop, J.L. Identification of hydrated silicate minerals on Mars using MRO-CRISM: Geologic context near Nili Fossae and implications for aqueous alteration. *J. Geophys. Res.* **2009**, *114*. [[CrossRef](#)]
16. Mangold, N.; Dehouck, E.; Fedo, C.; Forni, O.; Achilles, C.; Bristow, T.; Downs, R.T.; Frydenvang, J.; Gasnault, O.; L'Haridon, J.; et al. Chemical alteration offine-grained sedimentary rocks at Gale crater. *Icarus* **2019**, *321*, 619–631. [[CrossRef](#)]
17. Bishop, J.L.; Gross, C.; Danielsen, J.; Parente, M.; Murchie, S.L.; Horgan, B.; Wray, J.J.; Viviano, C.; Seelos, F.P. Multiple mineral horizons in layered outcrops at Mawrth Vallis, Mars, signify changing geochemical environments on early Mars. *Icarus* **2020**, *341*, 113634. [[CrossRef](#)]
18. Velde, B. Origin and mineralogy of clays. In *Clays and the Environment*; Springer: Berlin, Germany, 1995; p. 334.
19. Meunier, A.; Petit, S.; Ehlmann, B.L.; Dudoignon, P.; Westall, F.; Mas, A.; El Albani, A.; Ferrage, E. Magmatic precipitation as a possible origin of Noachian clays on Mars. *Nat. Geosci.* **2012**, *5*, 739–743. [[CrossRef](#)]
20. Galán, E.; Ferrell, R.E. Chapter 3—genesis of clay minerals. In *Developments in Clay Science*; Faïza, B., Gerhard, L., Eds.; Elsevier: Amsterdam, The Netherlands, 2017; pp. 83–126.
21. Wilson, M.J. The origin and formation of clay minerals in soils: Past, present and future perspectives. *Clay Min.* **1999**, *34*, 7–25. [[CrossRef](#)]
22. Schröder, C.; Bland, P.A.; Golombek, M.P.; Ashley, J.W.; Warner, N.H.; Grant, J.A. Amazonian chemical weathering rate derived from stony meteorite finds at Meridiani Planum on Mars. *Nat. Commun.* **2016**, *7*, 13459. [[CrossRef](#)]
23. Gitreau, M.; Flahaut, J. Record of low-temperature aqueous alteration of Martian zircon during the late Amazonian. *Nat. Commun.* **2019**, *10*, 2457. [[CrossRef](#)]
24. Banin, A.; Han, F.X.; Kan, I.; Cicelsky, A. Acidic volatiles and the Mars soil. *J. Geophys. Res.* **1997**, *102*, 13341–13356. [[CrossRef](#)]

25. Tosca, N.J.; McLennan, S.M.; Lindsley, D.H.; Schoonen, M.A. Acid-sulfate weathering of synthetic Martian basalt: The acid-fog model revisited. *J. Geophys. Res.* **2004**, *109*, E05003. [[CrossRef](#)]
26. Hurowitz, J.A.; McLennan, S.M. A ~3.5 Ga record of water-limited, acidic weathering conditions on Mars. *Earth Planet. Sci. Lett.* **2007**, *260*, 432–443. [[CrossRef](#)]
27. Zolotov, M.Y.; Mironenko, M.V. Timing of acid weathering on Mars: A thermodynamic-kinetic assessment. *J. Geophys. Res. Planets* **2007**, *112*, E07006. [[CrossRef](#)]
28. Bloise, A.; Cannata, C.B.; De Rosa, R. Hydrothermal Alteration of Etna Ash and Implications for Mars. *Minerals* **2020**, *10*, 450. [[CrossRef](#)]
29. Altheide, T.S.; Chevrier, V.F.; Noe Dobrea, E. Mineralogical characterization of acid weathered phyllosilicates with implications for secondary Martian deposits. *Geochim. Cosmochim. Acta* **2010**, *74*, 6232–6248. [[CrossRef](#)]
30. Gaudin, A.; Dehouck, E.; Grauby, O.; Mangold, N. Formation of clay minerals on Mars: Insights from long-term experimental weathering of olivine. *Icarus* **2018**, *311*, 210–223. [[CrossRef](#)]
31. Viennet, J.C.; Bultel, B.; Werner, S.C. Experimental reproduction of the martian weathering profiles argues for a dense Noachian CO<sub>2</sub> atmosphere. *Chem. Geol.* **2019**, *525*, 82–95. [[CrossRef](#)]
32. Dehouck, E.; Gaudin, A.; Mangold, N.; Lajaunie, L.; Dauzères, A.; Grauby, O.; Le Menn, E. Weathering of olivine under CO<sub>2</sub> atmosphere: A Martian perspective. *Geochim. Cosmochim. Acta* **2014**, *135*, 170–189. [[CrossRef](#)]
33. Smith, R.J.; Horgan, B.H.N.; Mann, P.; Cloutis, E.A.; Christensen, P.R. Acid weathering of basalt and basaltic glass: 2. Effects of microscopic alteration textures on spectral properties. *J. Geophys. Res. Planets* **2017**, *122*, 203–227. [[CrossRef](#)]
34. McCollom, T.M.; Robbins, M.; Moskowitz, B.; Berquó, T.S.; Jöns, N.; Hynek, B.M. Experimental study of acid-sulfate alteration of basalt and implications for sulfate deposits on Mars. *J. Geophys. Res. Planets* **2013**, *118*, 577–614. [[CrossRef](#)]
35. Marcucci, E.C.; Hynek, B.M. Laboratory simulations of acid-sulfate weathering under volcanic hydrothermal conditions: Implications for early Mars. *J. Geophys. Res. Planets* **2014**, *119*, 679–703. [[CrossRef](#)]
36. Horgan, B.H.N.; Smith, R.J.; Cloutis, E.A.; Mann, P.; Christensen, P.R. Acidic weathering of basalt and basaltic glass: 1. Near-infrared spectra, thermal infrared spectra, and implications for Mars. *J. Geophys. Res. Planets* **2017**, *122*. [[CrossRef](#)]
37. Peretyazhko, T.S.; Niles, P.B.; Sutter, B.; Morris, R.V.; Agresti, D.G.; Le, L.; Ming, D.W. Smectite formation in the presence of sulfuric acid: Implications for acidic smectite formation on early Mars. *Geochim. Cosmochim. Acta* **2018**, *220*, 248–260. [[CrossRef](#)]
38. Sætre, C.; Hellevang, H.; Riu, L.; Dypvik, H.; Pilorget, C.; Poulet, F.; Werner, S.C. Experimental hydrothermal alteration of basaltic glass with relevance to Mars. *Meteor. Planet. Sci.* **2018**, *54*, 357–378. [[CrossRef](#)]
39. Friedman, I.; Long, W. Volcanic glasses, their origins and alteration processes. *J. Non-Cryst. Solids* **1984**, *67*, 127–133. [[CrossRef](#)]
40. de la Fuente, S.; Cuadros, J.; Fiore, S.; Linares, J. Electron microscopy study of volcanic tuff alteration to illite-smectite under hydrothermal conditions. *Clays Clay Miner.* **2000**, *48*, 339–350. [[CrossRef](#)]
41. McSween, H.Y.; Taylor, G.J.; Wyatt, M.B. Elemental Composition of the Martian Crust. *Science* **2009**, *324*, 736–739. [[CrossRef](#)]
42. Leveille, R.; Datta, S. Lava tubes and basaltic caves as astrobiological targets on Earth and Mars: A review. *Planet. Space Sci.* **2010**, *58*, 592–598. [[CrossRef](#)]
43. Sauro, F.; Pozzobon, R.; Massironi, M.; De Berardinis, P.; Santagata, T.; Waele, J. Lava tubes on Earth, Moon and Mars: A review on their size and morphology revealed by comparative planetology. *Earth Sci. Rev.* **2020**, *209*, 103288. [[CrossRef](#)]
44. Chester, D.K.; Duncan, A.M.; Guest, J.E.; Kilburn, C.R.J. *Mount Etna: The Anatomy of a Volcano*; Chapman and Hall: London, UK, 1985; p. 404.
45. Bonaccorso, A.; Calvari, S.; Coltelli, M.; Del Negro, C.; Falsaperla, S. *Etna Volcano Laboratory*; American Geophysical Union: Washington, DC, USA, 2004; Volume 143.
46. Monaco, C.; de Guidi, G.; Ferlito, C. The Morphotectonic map of Mt.Etna. *Ital. J. Geosci.* **2010**, *129*, 408–428.
47. Tanguy, J.C.; Condomines, M.; Kieffer, G. Evolution of Mount Etna magma: Constraints on the present feeding system and eruptive mechanism. *J. Volcanol. Geoth. Res.* **1997**, *75*, 221–250. [[CrossRef](#)]
48. Branca, S.; Coltelli, M.; Groppelli, G. Geological evolution of a complex basaltic stratovolcano: Mount Etna, Italy. *Ital. J. Geosci.* **2011**, *130*, 265–291.

49. Gillot, P.Y.; Kieffer, G.; Romano, R. The evolution of Mount Etna in the light of potassium-argon dating. *Acta Vulcanol.* **1994**, *5*, 81–87.
50. De Beni, E.; Wijbrans, J.R.; Branca, S.; Coltelli, M.; GropPELLI, G. New results of  $^{40}\text{Ar}/^{39}\text{Ar}$  dating constrain the timing of transition from fissure-type to central volcanism at Mount Etna (Italy). *Terra Nova* **2005**, *17*, 292–298. [[CrossRef](#)]
51. Branca, S.; Coltelli, M.; De Beni, E.; Wijbrans, J. Geological evolution of Mount Etna volcano (Italy) from earliest products until the first central volcanism (between 500 and 100 ka ago) inferred from geochronological and stratigraphic data. *Int. J. Earth. Sci.* **2008**, *97*, 135–152. [[CrossRef](#)]
52. Corsaro, R.A.; Pompilio, M. Magma dynamics at Mount Etna. In *Etna—Volcano Laboratory*; Bonaccorso, A., Calvari, S., Coltelli, M., Del Negro, C., Falsaperla, S., Eds.; American Geological Union: Washington, DC, USA, 2004; pp. 91–110.
53. Kurokawa, H.; Kurosawa, K.; Usui, T. A lower limit of atmospheric pressure on early Mars inferred from nitrogen and argon isotopic compositions. *Icarus* **2018**, *299*, 443–459. [[CrossRef](#)]
54. Moore, D.M.; Reynolds, R.C., Jr. *X-ray Diffraction and the Identification and Analysis of Clay Minerals*, 2nd ed.; Oxford University Press: Oxford, UK, 1997; p. 378.
55. McSween, H.Y.; Ruff, S.W.; Morris, R.S.; Gellert, R.; Klingelhöfer, G.; Christensen, P.R.; McCoy, T.J.; Ghosh, A.; Moersch, J.M.; Cohen, B.A. Mineralogy of volcanic rocks in Gusev Crater, Mars: Reconciling Mössbauer, Alpha Particle X-Ray Spectrometer, and Miniature Thermal Emission Spectrometer spectra. *J. Geophys. Res.* **2008**, *113*, E06S04. [[CrossRef](#)]
56. Cousin, A.; Sautter, V.; Payré, V.; Forni, O.; Mangold, N.; Gasnault, O.; le Deit, L.; Johnson, J.; Maurice, S.; Salvatore, M.; et al. Classification of igneous rocks analyzed by chemcam at gale crater, Mars. *Icarus* **2017**, *288*, 265–283. [[CrossRef](#)]
57. Cardinale, M.; Pozzobon, R.; Tangari, A.C.; Runyon, K.; Di Primio, M.; Marinangeli, L. Reconstruction of the sand transport pathways and provenance in Moreux crater, Mars. *Planet Space Sci.* **2019**, *181*, 104788. [[CrossRef](#)]
58. Pelkey, S.M.; Mustard, J.F.; Murchie, S.; Clancy, R.T.; Wolff, M.; Smith, M.; Milliken, R.; Bibring, J.P.; Gendrin, A.; Poulet, F.; et al. CRISM multispectral summary products: Parameterizing mineral diversity on Mars from reflectance. *J. Geophys. Res.* **2007**, *112*, E8. [[CrossRef](#)]
59. Larsen, N.; Svendsen, S.H.; Knudsen, B.M.; Voigt, C.; Weisser, C.; Kohlmann, A.; Schreiner, J.; Mauersberger, K.; Deshler, T.; Kroger, C.; et al. Microphysical mesoscale simulations of polar stratospheric cloud formation constrained by in situ measurements of chemical and optical cloud properties. *J. Geophys. Res.* **2002**, *107*, 8301. [[CrossRef](#)]
60. Grotzinger, J.P. Analysis of surface materials by the Curiosity Mars Rover. *Science* **2013**, *341*, 1475. [[CrossRef](#)]
61. Kawano, M.T.; Katsutoshi, T.; Yasushi, S. Analytical electron microscopic study of the non crystalline products formed at early weathering stages of volcanic glass. *Clays Clay Miner.* **1997**, *45*, 440–447. [[CrossRef](#)]
62. Hazen, R.M.; Sverjensky, D.A.; Azzolini, D.; Bish, D.L.; Elmore, S.C.; Hinnov, L.; Milliken, R.E. Clay mineral evolution. *Am. Miner.* **2013**, *98*, 2007–2029. [[CrossRef](#)]
63. Tangari, A.C.; Scarciglia, F.; Piluso, E.; Marinangeli, L.; Pompilio, L. Role of weathering of pillow basalt, pyroclastic input and geomorphic processes on the genesis of the Monte Cerviero upland soils (Calabria, Italy). *Catena* **2018**, *171*, 299–315. [[CrossRef](#)]
64. Adamo, P.; Violante, P.; Wilson, M.J. Tubular and spheroidal halloysite in pyroclastic deposits in the area of the Roccamonfina volcano (Southern Italy). *Geoderma* **2001**, *99*, 295–316. [[CrossRef](#)]
65. Ugolini, F.C.; Dahlgren, R.A. Soil development in volcanic ash. *Glob. Environ. Res.* **2002**, *6*, 69–81.
66. Rasmussen, C.; Dahlgren, R.A.; Southard, R.J. Basalt weathering and pedogenesis across an environmental gradient in the southern Cascade Range, California, USA. *Geoderma* **2010**, *154*, 473–485. [[CrossRef](#)]
67. Egli, M.; Nater, M.; Mirabella, A.; Raimondi, S.; Plötze, M.; Alioth, L. Clay minerals, oxyhydroxide formation, element leaching and humus development in volcanic soils. *Geoderma* **2008**, *143*, 101–114. [[CrossRef](#)]
68. Liotta, M.; Paonita, A.; Caracausi, A.; Martelli, M.; Rizzo, A.; Favara, R. Hydrothermal processes governing the geochemistry of the crater fumaroles at Mount Etna volcano (Italy). *Chem. Geol.* **2010**, *278*, 92–104. [[CrossRef](#)]
69. Liotta, M.; D’Alessandro, W.; Bellomo, S.; Brusca, L. Volcanic plume fingerprint in the groundwater of a persistently degassing basaltic volcano: Mt Etna. *Chem. Geol.* **2016**, *433*, 68–80. [[CrossRef](#)]

70. Chadwick, O.A.; Gavenda, R.T.; Kelly, E.F.; Ziegler, K.; Olso, C.G.; Elliott, W.C.; Hendricks, D.M. The impact of climate on the biogeochemical functioning of volcanic soils. *Chem. Geol.* **2003**, *202*, 195–223. [[CrossRef](#)]
71. Kawano, M.; Tomita, K. Formation of allophane and beidellite during hydrothermal alteration of volcanic glass below 200 °C. *Clays Clay Min.* **1992**, *40*, 666–674. [[CrossRef](#)]
72. Mirabella, A.; Egli, M.; Raimondi, S.; Giaccai, D. Origin of clay minerals in soils on pyroclastic deposits in the island of Lipari (Italy). *Clays Clay Min.* **2005**, *53*, 409–421. [[CrossRef](#)]
73. Garcia-Romero, E.; Vegas, J.; Baldonado, J.L.; Marfil, R. Clay minerals as alteration products in basaltic volcanoclastic deposits of La Palma (Canary Islands, Spain). *Sediment. Geol.* **2005**, *174*, 237–253. [[CrossRef](#)]
74. Kawano, M.; Tomita, K. Experimental study on the formation of zeolites from obsidian by interaction with NaOH and KOH solutions at 150 and 200 °C. *Clays Clay Miner.* **1997**, *45*, 365–377. [[CrossRef](#)]
75. Evans, B.W.; Hattori, K.H.; Baronnet, A. Serpentinite: What, why, where? *Elements* **2013**, *9*, 99–106. [[CrossRef](#)]
76. Geptner, A.R.; Ivanovskaya, T.A.; Pokrovskaya, E.V. Hydrothermal fossilization of microorganisms at the Earth's surface in Iceland. *Lithol. Miner. Resour.* **2005**, *40*, 505–520. [[CrossRef](#)]
77. Piochi, M.; Kilburn, C.R.J.; Di Vito, M.A.; Mormone, A.; Tramelli, A.; Troise, C.; de Natale, G. The volcanic and geothermally active Campi Flegrei caldera: An integrated multidisciplinary image of its buried structure. *Int. J. Earth Sci.* **2014**, *103*, 401–421. [[CrossRef](#)]
78. Gresse, M.; Vandemeulebrouck, J.; Byrdina, S.; Chiodini, G.; Roux, P.; Rinaldi, A.P.; Wathelet, M.; Ricci, T.; Letort, J.; Petrillo, Z.; et al. Anatomy of a fumarolic system inferred from a Multiphysics approach. *Sci. Rep.* **2018**, *8*, 7580–7590. [[CrossRef](#)] [[PubMed](#)]
79. Shevenell, L.; Goff, F. Evolution of hydrothermal waters at Mount St. Helens, Washington, USA. *J. Volcanol. Geotherm. Res.* **1995**, *69*, 73–94. [[CrossRef](#)]
80. Pirajno, F. Subaerial hot springs and near-surface hydrothermal mineral systems past and present, and possible extraterrestrial analogues. *Geosci. Front.* **2020**, *11*, 1549–1569. [[CrossRef](#)]
81. Triana, J.M.R.; Herrera, J.F.R.; Rios, R.C.A.; Castellanos, O.M.A.; Henao, J.A.M.; Williams, C.D.; Roberts, C.L. Natural zeolites filling amygdales and veins in basalts from the British Tertiary igneous Province on the Isle of Skye, Scotland. *Earth Sci. Res. J. Petrol.* **2012**, *16*, 41–53.
82. Le Deit, L.; Flahaut, J.; Quantin, C.; Hauber, E.; Mège, D.; Bourgeois, O.; Gurgurewicz, J.; Massé, M.; Jaumann, R. Extensive surface pedogenic alteration of the Martian Noachian crust suggested by plateau phyllosilicates around Valles Marineris. *J. Geophys. Res.* **2012**, *117*, E00J05. [[CrossRef](#)]
83. Yen, A.S.; Morris, R.V.; Clarck, B.C.; Gellert, R.A.; Knudson, T.; Squyres, S.; Mittlefehldt, D.W.; Ming, D.W.; Arvidson, R.; McCoy, T.; et al. Hydrothermal processes at Gusev Crater: An evaluation of Paso Robles Class soils. *J. Geophys. Res.* **2008**, *113*, E06S10. [[CrossRef](#)]
84. McGlynn, I.O.; Fedo, C.M.; McSween, H.Y., Jr. Soil mineralogy at the Mars Exploration Rover landing sites: An assessment of the competing roles of physical sorting and chemical weathering. *J. Geophys. Res.* **2012**, *117*, 1006. [[CrossRef](#)]
85. Nazari-Sharabian, M.; Aghababaei, M.; Karakouzian, M.; Karami, M. Water on Mars—A Literature Review. *Galaxies* **2020**, *8*, 40. [[CrossRef](#)]
86. Pondrelli, M.; Rossi, A.P.; Platz, T.; Ivanov, A.; Marinangeli, L.; Baliva, A. Geological, geomorphological, facies and allostratigraphic maps of the Eberwalde fan delta. *Planet. Space Sci.* **2011**, *59*, 1166–1178. [[CrossRef](#)]
87. Le Deit, L.; Mangold, N.; Forni, O.; Schröder, S.; Stack, K.M.; Sumner, D.; Fisk, M.; Dromart, G.; Blaney, D.; Fabre, C.; et al. The potassic sedimentary rocks in Gale Crater, Mars, as seen by ChemCam on board Curiosity. *J. Geophys. Res. Planets* **2016**, *121*, 784–804. [[CrossRef](#)]
88. Fernández-Remolar, D.C.; Morris, R.V.; Gruener, J.E.; Amils, R.; Knoll, A.H. The Río Tinto Basin, Spain: Mineralogy, sedimentary geobiology and implications for interpretation of outcrop rocks at Meridiani Planum, Mars. *Earth Planet. Sci. Lett.* **2005**, *240*, 149–167. [[CrossRef](#)]
89. Fernández-Remolar, D.C.; Prieto-Ballesteros, O.; Gómez-Ortíz, D.; Fernández-Sampedro, M.; Sarrazin, P.; Gailhanou, M.; Amils, R. Río Tinto sedimentary mineral assemblages: A terrestrial perspective that suggests some formation pathways of phyllosilicates on Mars. *Icarus* **2011**, *211*, 114–138. [[CrossRef](#)]
90. Kyle, J.E.; Schroeder, P.A. Role of smectite in siliceous-sinter formation and microbial-texture preservation: Octopus Spring, Yellowstone National Park, Wyoming, USA. *Clay Clay Miner.* **2007**, *55*, 189–199. [[CrossRef](#)]
91. Ruff, S.W.; Campbell, K.A.; Van Kranendonk, M.J.; Rice, M.S.; Farmer, J.D. The case for ancient hot springs in Gusev crater, Mars. *Astrobiology* **2020**, *20*, 475–499. [[CrossRef](#)]

92. Costello, L.J.; Filiberto, J.; Crandall, J.R.; Potter-McIntyre, S.L.; Schwenzer, S.P.; Miller, M.A.; Hummer, D.R.; Olsson-Francis, K.; Perl, S. Habitability of hydrothermal systems at Jezero and Gusev Craters as constrained by hydrothermal alteration of a terrestrial mafic dike. *Geochemistry* **2020**, *80*, 125613. [[CrossRef](#)]
93. Carter, J.; Poulet, F. Orbital identification of clays and carbonates in Gusev crater. *Icarus* **2012**, *219*, 250–253. [[CrossRef](#)]
94. Clark, B.C.; Arvidson, R.E.; Gellert, R.; Morris, R.V.; Ming, D.W.; Richter, L.; Ruff, S.W.; Michalski, J.R.; Farrand, W.H.; Yen, A.; et al. Evidence for montmorillonite or its compositional equivalent in ColumbiaHills, Mars. *J. Geophys. Res.* **2007**, *112*, E06S01.
95. Catling, D.C. Mars atmosphere: History and surface interactions. In *Encyclopedia of the Solar System*; Spohn, T., Breur, D., Johnson, T.V., Eds.; Elsevier: Amsterdam, The Netherlands, 2014; pp. 343–357.
96. Hurowitz, J.A.; McLennan, S.M.; Tosca, N.J.; Arvidson, R.E.; Michalski, J.R.; Ming, D.W.; Schröder, C.; Squyres, S.W. In-situ and experimental evidence for acidic weathering of rocks and soils on Mars. *J. Geophys. Res.* **2006**, *111*, E02S19. [[CrossRef](#)]
97. McAdam, A.C.; Zolotov, M.Y.; Mironenko, M.V.; Sharp, T.G. Formation of silica by low-temperature acid alteration of Martian rocks: Physical-chemical constraints. *J. Geophys. Res.* **2008**, *113*, 08003. [[CrossRef](#)]
98. Squyres, S.W.; Arvidson, R.E.; Ruff, S.; Gellert, R.; Morris, R.V.; Ming, D.W.; Crumpler, L.; Farmer, J.D.; Des Marais, D.J.; Yen, A.; et al. Detection of silica-rich deposits on mars. *Science* **2008**, *320*, 1063–1067. [[CrossRef](#)]
99. Halevy, I.; Head, J.W., III. Episodic warming of early Mars by punctuated volcanism. *Nat. Geosci.* **2014**, *7*, 865–868. [[CrossRef](#)]
100. Gaudin, A.; Dehouck, E.; Mangold, N. Evidence for weathering on early Mars from a comparison with terrestrial weathering profiles. *Icarus* **2011**, *216*, 257–268. [[CrossRef](#)]

**Publisher's Note:** MDPI stays neutral with regard to jurisdictional claims in published maps and institutional affiliations.



© 2020 by the authors. Licensee MDPI, Basel, Switzerland. This article is an open access article distributed under the terms and conditions of the Creative Commons Attribution (CC BY) license (<http://creativecommons.org/licenses/by/4.0/>).